3.3.1 Space truncation errors. Computational phase speed. Second and fourth order schemes.

It is convenient to separate the truncation errors in a discretized model into space truncation errors and time truncation errors. For explicit finite difference models, the errors introduced by space truncation tend to dominate the total forecast errors because for "weather waves" the time step and the Courant number used are much smaller than would be required to physically resolve the frequency. Let's neglect for the moment time truncation errors and consider the wave equation $\frac{\partial U}{\partial t} = -c\frac{\partial U}{\partial x}$ discretized only in space.

If we approximate $\frac{\partial U}{\partial x}$ using space centered differences:

$$\delta_{2x}U_j = \frac{U_{j+1} - U_{j-1}}{2\Delta x} = U_x + \frac{\Delta x^2}{6}U_{xxx} + \frac{\Delta x^4}{120}U_{xxxxx} + HOT$$

$$= U_x + A\Delta x^2 + B\Delta x^4 + \ldots$$

(1)

If instead of the closest neighboring points j+1, j-1, we use the points j+2, j-2, so instead of Δx we have $2\Delta x$:

$$\delta_{4x}U_j = \frac{U_{j+2} - U_{j-2}}{4\Delta x} = U_x + 4A\Delta x^2 + 16B\Delta x^4 + \ldots$$

(2)
This is also a second order scheme, but the second order truncation errors are 4 times as large. We can now eliminate from (1) and (2) the term $A\Delta x^2$, and obtain

$$\frac{4}{3}\delta_{2x}U_j - \frac{1}{3}\delta_{4x}U_j = U_x - 4B\Delta x^4 + \ldots \qquad (3)$$

Now (3) is a **fourth order** approximation of the space derivative. So

$$\frac{dU_j}{dt} = -c\delta_{2x}U_j \qquad (4)$$

is a **second order FDE** and

$$\frac{dU_j}{dt} = -c\left\{\frac{4}{3}\delta_x U_j - \frac{1}{3}\delta_{2x}U_j\right\} \qquad (5)$$

is a **fourth order FDE**.

Assume solutions of the form

$$U_j(t) = Ae^{ik(x_j - c't)} = Ae^{i(kx_j - \nu' t)} \qquad (6)$$

where c' is the computational phase speed, and ν' the computational frequency, so

$$\frac{dU_j}{dt} = -i\nu' U_j \ .$$

Making use of $\delta_{2x} U_j = i \frac{\sin k\Delta x}{\Delta x} U_j$, and replacing in (4) and (5) we find that for second order differences,

$$c'_2 = \frac{\sin k\Delta x}{k\Delta x} c \qquad (7)$$

and for fourth order differences,

$$c'_4 = c \left\{ \frac{4}{3} \frac{\sin k\Delta x}{k\Delta x} - \frac{1}{3} \frac{\sin 2k\Delta x}{2k\Delta x} \right\} . \qquad (8)$$

Note that (7) and (8) imply that the phase speed is always underestimated by space finite differences.

For the smallest possible wavelength, L=2Δx, kΔx=π, the computational phase speed is zero for both 2nd and 4th order differences: the shortest waves don't move at all! (Fig.3.7)

For L=4Δx, kΔx=π/2, a much more accurate approximation is obtained with 4th order than with 2nd order differences: $c'_2 = 0.64c,\ c'_4 = 0.85c$, and the 4th order advantage becomes even better for longer waves: for L=8Δx, $c'_2 = 0.90c,\ c'_4 = 0.99c$.

Computational phase speed and group velocity

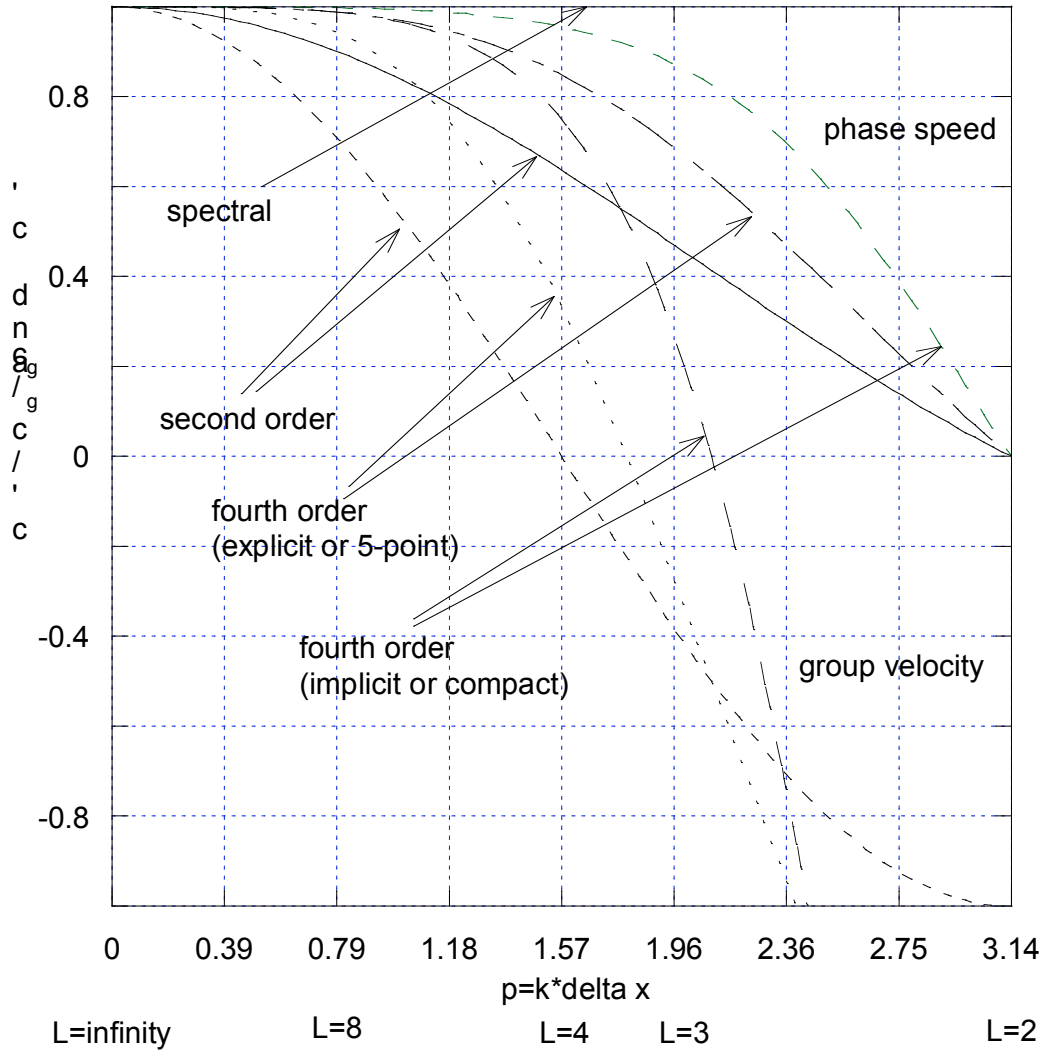

We can also compute the **computational group velocity** $\partial \nu' / \partial k$ where

$$\nu' = c'k = c\frac{\sin k\Delta x}{\Delta x} \tag{3.1}$$

for 2nd order differences. Then,

$$\frac{\partial \nu'}{\partial k} = c\cos k\Delta x \tag{3.2}$$

for second order differences. Therefore, for the shortest waves, L=2Δx, kΔx=π, with both second and fourth order differences the energy moves in the opposite direction as the real group velocity (equal to the phase speed c): $c_g' = -c_g$.

Fig. 3.7 shows the computational phase speed and group velocity for 2nd and 4th order differences. As a result of the negative group velocity, space centered FDE's of the wave equation tend to leave a trail of short-wave computational noise upstream of where the real perturbation should be. This problem is greatly reduced using more recent schemes such as those of Takacs (1985) and Smolarkiewicz and Grawoski (1990).

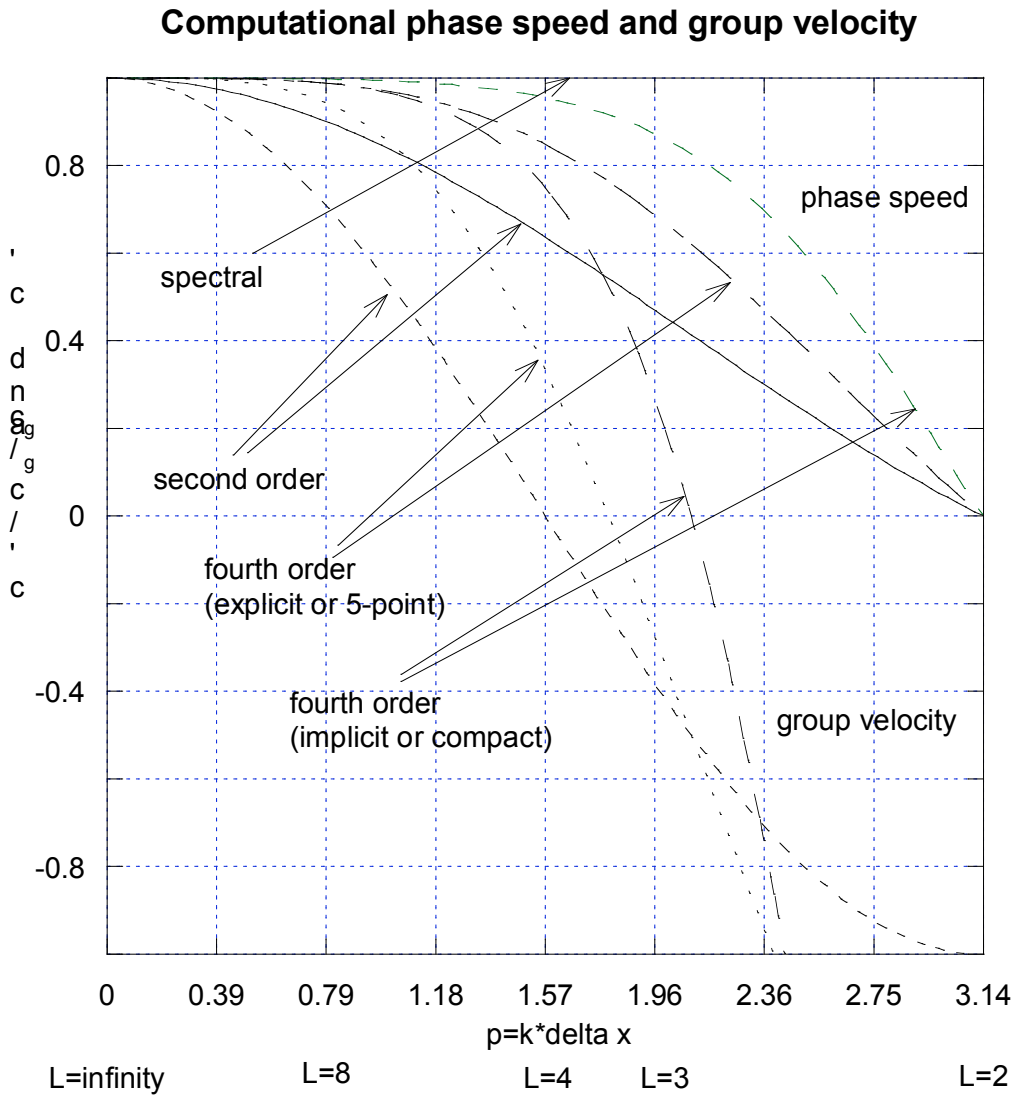

Fig. 3.7: Ratio of the computational to the physical phase speed c'/c and group velocity c_g'/c_g for a simple wave equation, neglecting time truncation errors, for second order, fourth order explicit and implicit and spectral schemes.

A second type of 4th order finite difference scheme, known as **compact** or **implicit** 4th order scheme, can be obtained by again making use of

$$\delta_{2x}U_j = \frac{U_{j+1} - U_{j-1}}{\Delta x} = U_x + \frac{\Delta x^2}{6}U_{xxx} + \frac{\Delta x^4}{120}U_{xxxxx} + HOT$$
$$= U_x + A\Delta x^2 + B\Delta x^4 + \ldots$$

Now we replace the third derivative U_{xxx} in the truncation error for the centered differences by its finite difference approximation (second derivative of the first derivative):

$$U_{xxxj} \approx (U_{xj+1} - 2U_{xj} + U_{xj-1}) / (\Delta x)^2 + O(\Delta x)^2 .$$

The new 4th order scheme becomes

$$U_{xj+1} + 4U_{xj} + U_{xj-1} = 6\frac{U_{j+1} - U_{j-1}}{2\Delta x} \qquad (11)$$

It is called "compact" because it involves only the point *j* and its closest neighbors, and "implicit" because (11) results in a system of (tridiagonal) equations for the x-derivative, rather than an explicit estimate as (4) or (5).

Exercise: Show that with this scheme, the finite difference space derivative for a Fourier component with wave number *k* is given by

$$U_x \simeq U \frac{i \sin k\Delta x}{\Delta x} \frac{6}{4 + 2\cos k\Delta x},$$

$$\frac{dU_j}{dt} = -icU_j \frac{\sin k\Delta x}{\Delta x} \frac{6}{4 + 2\cos k\Delta x} =$$

so that

$$= -ic'_{4I} kU_j = -iv'_{4I} U_j$$

The computational phase speed is therefore

$$c'_{4I} = \frac{\sin k\Delta x}{k\Delta x} \frac{6}{4 + 2\cos k\Delta x} c \qquad (12)$$

For $L=4\Delta x$, $k\Delta x=\pi/2$, the phase speed is $c'_{l4}=0.955c$, considerably better even than the regular 4th order differences phase speed.

The group velocity for this scheme,

$$\frac{\partial v'_{4I}}{\partial k} = [\frac{6\cos k\Delta x}{4 + 2\cos k\Delta x} + \frac{2\sin k\Delta x}{(4 + 2\cos k\Delta x)^2}]c \qquad (13)$$

is already positive for $L=4\Delta x$ (Fig.3.7).

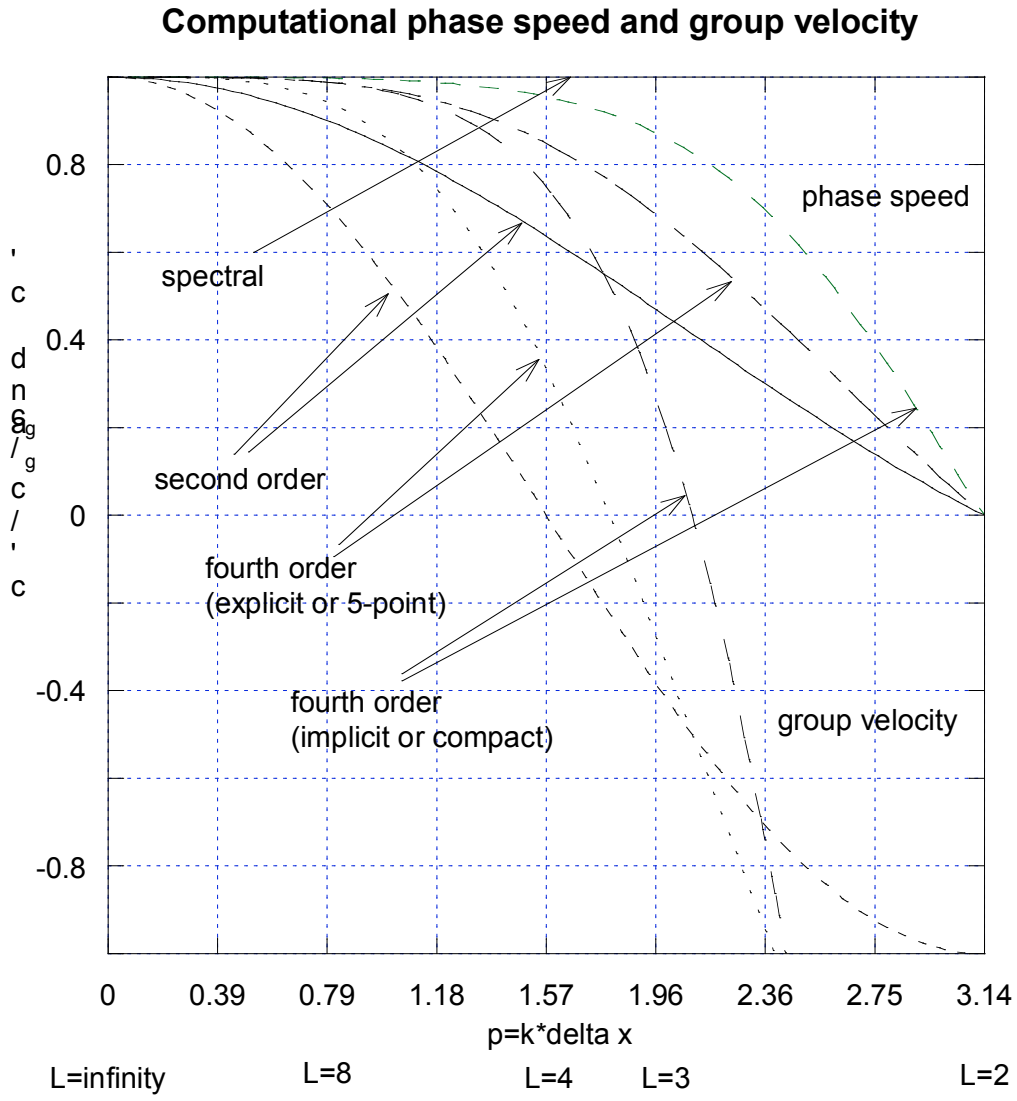

For implicit schemes where one is already solving a tri-diagonal equation, this compact 4th order scheme, which has accuracy equivalent to linear finite elements, is very accurate and involves little additional computational cost. The compact scheme is similar to Galerkin finite element approximation to space derivatives (Durran, 1999).

3.3.2: Galerkin and Spectral space representation

The use of spatial finite differences, as we saw in the previous section, introduces errors in the space derivatives, resulting in a computational phase speed slower than the true phase speed, especially for short waves.

The Galerkin approach to ameliorate this problem is to perform the space discretization using a sum of basis functions

$$U(x,t) = \sum_{k=1}^{K} A_k(t)\varphi(x)$$

Then, the residual (truncation error) $R(U)$

$$R(U) = \frac{\partial U}{\partial t} + F(U)$$

of the original PDE $\frac{\partial u}{\partial t} + F(u) = 0$

is required to be orthogonal to the basis functions $\varphi(x)$.

The space derivatives are computed directly from the known $d\varphi(x)/dx$.

This procedure leads to a set of ordinary differential equations for the coefficients $A_k(t)$.

If the basis functions chosen for the discretization are orthogonal and satisfy the boundary conditions, the derivation becomes simpler. The use of **local** basis functions (e.g., $\varphi_i(x)$ a piecewise linear function equal to 1 at a grid point *i* and zero at the neighboring points) gives rise to the **finite element method**, with accuracy similar to that of the compact (implicit) 4th order scheme.

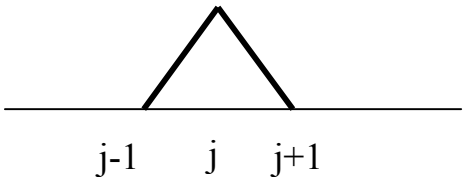

Local linear basis function $\varphi_j(x)$

Another popular type of Galerkin approach is the use of a **global spectral expansion** for the space discretization, which allows computing the space derivatives analytically rather than numerically. In one dimension, periodic boundary conditions suggest the use of complex Fourier series as a basis.

Consider JM grid points in a periodic domain of length L, and scale x by multiplying it by (2π/L). If we use discrete complex Fourier series truncated to include wavenumbers up to K, the spectral representation is:

$$U(x_j,t) = \sum_{k=-K}^{K} A_k(t) e^{ikx_j} \quad . \qquad (14)$$

where $A_{-k}(t) = A_k{}^*(t)$,

and the star represents the complex conjugate.

Alternatively, (14) can be written using real Fourier series as

$$U(x_j,t) = a_0 + \sum_{k=1}^{K} a_k \cos(kx) + \sum_{k=1}^{K} b_k \sin(kx) \qquad (15)$$

where $A_k(t) = \frac{a_k}{2} - i\frac{b_k}{2}, k > 0; \quad A_0 = a_0$

There are 2K+1 distinct real coefficients that are determined by

$$A_k(t) = \frac{1}{JM} \sum_{j=0}^{JM-1} U(x_j,t) e^{-ikx_j} \qquad (16)$$

Here we have used the orthogonality property

$$\frac{1}{JM} \sum_{j=1}^{JM} e^{-ikx_j} e^{ilx_j} = \delta_{kl} = \begin{cases} 1 & \text{if } k = l \\ 0 & \text{otherwise} \end{cases} \qquad (17)$$

If JM=2K+1, the grid representation (left hand side of (14)) and the spectral representation (right hand side of (14)) contain the same number of degrees of freedom, and the same information.

Then, in the wave equation $\frac{\partial U}{\partial t} = -c\frac{\partial U}{\partial x}$, we can discretize U in space as in (14) and compute the space derivative analytically:

$$\frac{\partial U(x,t)}{\partial x} = \sum_{k=-K}^{K} ikA_k(t)e^{ikx} \qquad (3.3)$$

If we neglect the time discretization errors, as before, and assume solutions of the form $U(x,t) = Ae^{ik(x-c't)}$, we find that c'=c, i.e., the computational phase speed I a spectral method is *equal* to the true speed (Fig.3.7). *The space discretization based on a spectral representation is extremely accurate* (the space truncation errors are of "infinite" order). This is because the space derivatives are computed analytically, not numerically, as done in finite differences.

If the PDE is nonlinear, for example $\frac{\partial U}{\partial t} = -U\frac{\partial U}{\partial x}$, then both the grid-point ("physical space") representation and the spectral representation are very useful:

The derivatives $\frac{\partial U}{\partial x}$ are computed efficiently and accurately in spectral space, whereas nonlinear products $U\frac{\partial U}{\partial x}$ are computed efficiently in physical space.

This is the so-called **transform method** used for spectral models: the space derivative is computed in spectral space, then U is transformed back into grid space, and the product $U_j\left(\frac{\partial U}{\partial x}\right)_j$ is computed locally in grid space.

We will see later that in order to avoid nonlinear instability introduced by aliasing of wavenumbers beyond K that appear in quadratic terms, the grid representation requires about 3/2 as many points as the minimum number of points required for a linear transform (JM=2K+1). For this reason the new values of U at time (n+1)Δt are usually stored in their spectral representation, which is more compact.

We can use von Neuman's criterion to determine the maximum time step allowed for stability using, for example, the leap-frog time scheme. The FDE is

$$\frac{U^{n+1}-U^{n-1}}{2\Delta t}=-ikcU^n \qquad (3.4)$$

Assuming solutions for the wave equation of the form $U^n = \rho^n e^{ikx}$, we obtain that the amplification factor is

$$\rho = -ikc\Delta t \pm \sqrt{1 - k^2 c^2 \Delta t^2},$$

In order to have $|\rho| \leq 1$ we need to satisfy the stability condition .

$$(kc\Delta t)^2 \leq 1 \qquad (3.5)$$

Since the highest wavenumber present corresponds to L=2Δx, the stability criterion for spectral models is therefore

$$\left|\frac{c\Delta t}{\Delta x}\right| \leq \frac{1}{\pi}.$$

Recall that for second order differences the stability criterion was $\left|\frac{c\Delta t}{\Delta x}\right| \leq 1$

So, the stability criterion is more restrictive for spectral models than for finite difference models, but this is compensated by the fact that the accuracy, especially for shorter waves, is much higher, and therefore fewer short waves need to be included (Fig.3.7).

The basis functions used in spectral methods are usually the eigensolutions of the Laplace equation. In a rectangular domain, they are sines and cosines (e.g., the Regional Spectral Model, Juang et al, 1999). On a circular plate, one would instead use Bessel functions.

Global atmospheric models use as basis functions spherical harmonics, which are the eigenfunctions of the Laplace equation on the sphere:

$$\nabla^2 Y_n^m = \frac{1}{a^2}\left[\frac{1}{\cos^2\varphi}\frac{\partial^2 Y_n^m}{\partial\lambda^2} + \frac{1}{\cos\varphi}\frac{\partial}{\partial\varphi}\left(\cos\varphi\frac{\partial Y_n^m}{\partial\varphi}\right)\right] =$$

$$= \frac{-n(n+1)}{a^2} Y_n^m \qquad (21)$$

The spherical harmonics are products of Fourier series in longitude and associated Legendre polynomials in latitude:

$$Y_n^m(\lambda,\phi) = P_n^m(\mu)e^{im\lambda}, \qquad (22)$$

where $\mu = \sin(\phi)$ m is the zonal wavenumber and n is the "total" wavenumber in spherical coordinates (as suggested by the Laplace equation). P_n^m are the associated Legendre polynomials in x=cos θ, where $\theta = \pi/2 - \phi$ θ=π/2-φ is the colatitude. For example, the $P_0^0=1$; $P_1^0=\cos\theta$; $P_1^1=\sin\theta$; $P_2^0=1/2\,(3\cos^2\theta-1)$; $P_2^1=3\sin\theta\cos\theta$; $P_2^1=3\sin^2\theta$;…

Using "triangular" truncation

$$U(\lambda,\varphi,t)=\sum_{n=0}^{N}\sum_{m=-n}^{n}U_n^m(t)Y_n^m(\lambda,\varphi) \qquad (23)$$

the spatial resolution is uniform throughout the sphere. This has a major advantage over finite differences based on a latitude-longitude grid, where the convergence of the meridians at the poles requires very small time steps.

Although there are solutions for this “pole problem” for finite differences, the natural approach to solve the pole problem for global models is the use of spherical harmonics. Williamson and Laprise (1998) provide a comprehensive description of numerical methods for global models.

Fig. 3.8a (reproduced from Williamson and Laprise, 1998) shows the shape of three spherical harmonics with total wavenumber n=6, and zonal wavenumber m=0, 3 and 6. Note that the distance between neighboring maxima and minima is similar for the 3 harmonics, and is associated with the “total” (2-dimensional) wavenumber n.

Fig. 3.8b and c (also reproduced from Williamson and Laprise, 1998) show that the amplitude of the Legendre polynomials for high zonal wavenumbers are indeed suppressed near the poles. This suppression eliminates the need for small time steps due to the convergence of the meridians in the poles, which are not singular points spectral models.

Fig. 3.8. Illustration of the characteristics of spherical harmonics, from Williamson and Laprise (1998). A) Depiction of three spherical harmonics with total wave number n=6. Left, zonal wave number m=0; center, m=3; right, m=6. Note that n is associated with the total wavelength (twice the distance between a maximum and a minimum), which is the same for the three figures.
B) and C) Amplitude of Legendre polynomials for different combinations of m and n showing how high zonal wave numbers are suppressed near the poles, so that the horizontal resolution is uniform when using a spectral representation with triangular truncation.

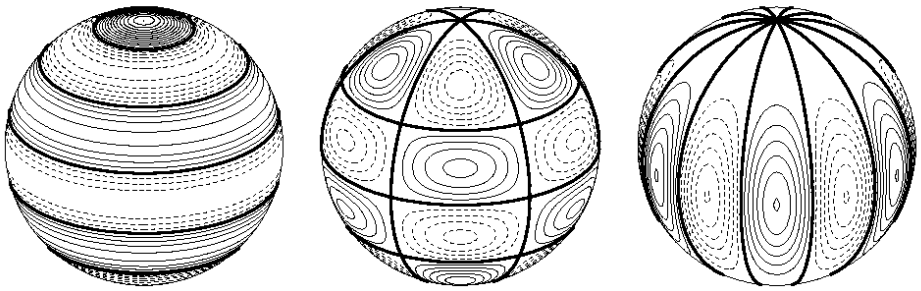

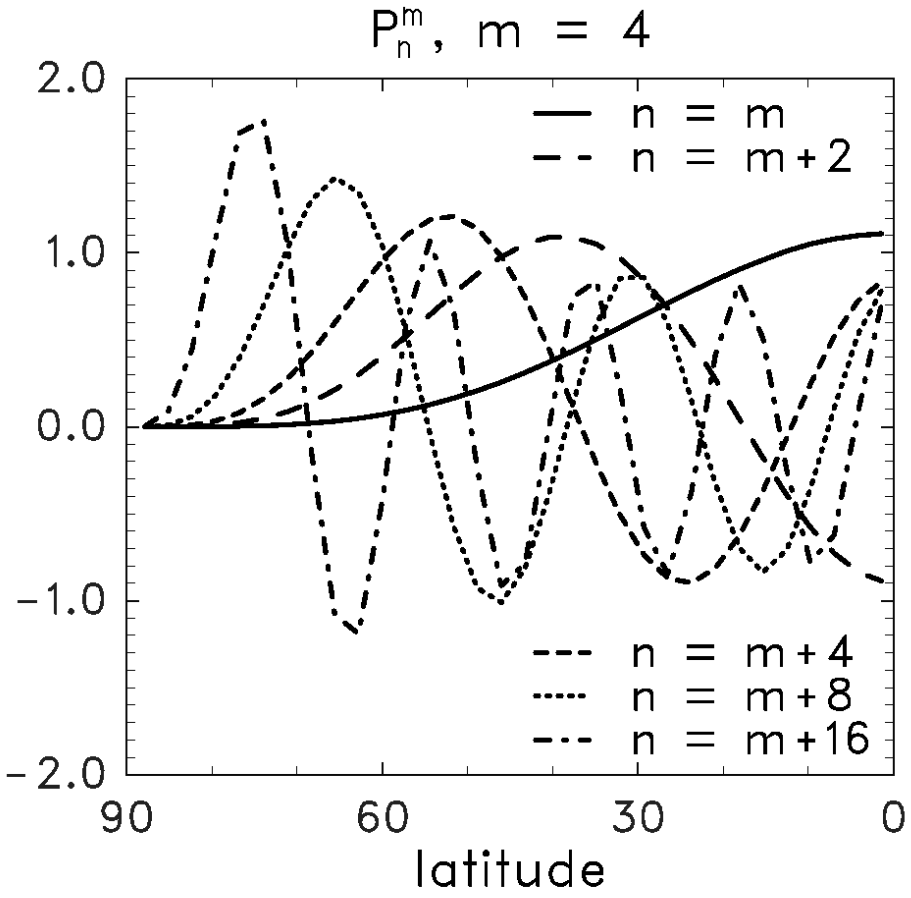
P_n^m, m = 4
2.0
1.0
0.0
−1.0
−2.0
90
60
30
0
latitude
n = m
n = m+2
n = m+4
n = m+8
n = m+16

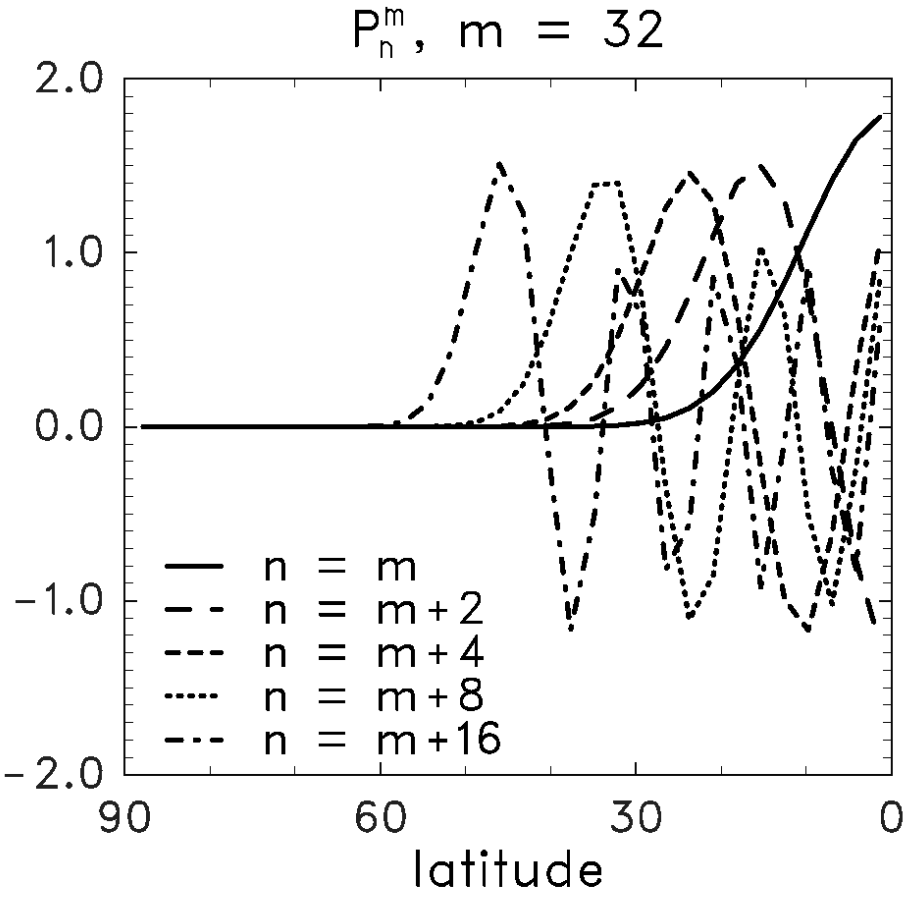
P_n^m, m = 32
2.0
1.0
0.0
-1.0
-2.0
90
60
30
0
latitude
n = m
n = m+2
n = m+4
n = m+8
n = m+16